Fouling Elimination of PTFE Membrane under Precoagulation Process Combined with Ultrasound Irradiation

Meng-Wei Wan, Ph.D.[1]; Hui-Ling Yang, Ph.D.[2]; Cheng-Hung Chang[3]; Febelyn Reguyal[4]; and Chi-Chuan Kan, Ph.D.[5]

Abstract: Precoagulation is one of the effective pretreatments in membrane filtration. This process mitigates membrane fouling, which is the major drawback of membrane technology in drinking water and wastewater treatment. This study investigated the effects of precoagulation under different coagulation mechanisms on membrane fouling. Use of ultrasound in polytetrafluoroethylene (PTFE) membrane cleaning was also evaluated. In precoagulation, synthetic raw water was precoagulated using aluminum sulfate at different coagulation mechanisms, named electrostatic patch effect (EPE), charge neutralization (CN), and sweep flocculation (SW). Flocs produced from different coagulation mechanisms exhibited different sizes, structures, and strengths. Likewise, the fouling type generated from each mechanism was demonstrated as pore blocking for EPE, cake formation for SW, and combination phenomenon for CN. Moreover, this study indicated that the membrane flux was enhanced in the sequence of EPE > CN > SW. The flux recovery rate after ultrasonic cleaning was in the sequence of SW > CN > EPE. Finally, this study evidenced that the floc characteristics from various coagulation mechanisms affected membrane performance, fouling types, and ultrasonic cleaning efficiency. **DOI: 10.1061/(ASCE)EE.1943-7870.0000406.**

CE Database subject headings: Coagulation; Filtration; Ultrasonic methods; Wastewater management.

Author keywords: Coagulation; Microfiltration; Ultrasonic cleaning; Floc characteristic.

Introduction

In recent years, membrane technology has been widely used in water and wastewater treatment, including microfiltration (MF), ultrafiltration (UF), nanofiltration (NF), and reverse osmosis (RO) (Bergamasco 2009; Kweon et al. 2009). Compared with conventional methods, membrane technologies could provide more efficient but less economical water treatment process (Strathmann 1976). High operating costs and membrane fouling were considered as the limitations for their applications. Many researchers have recently devoted their efforts in significantly reducing the operation cost for membrane systems. However, the fouling problem remains to be the major obstacle to membrane technology (Lamminen et al. 2004).

Fouling problem reduces permeability of a membrane attributable to the accumulation of colloids, particles, macromolecules, and salts on the membrane surface, which consequently resulted in flux reduction. This phenomenon increases the maintenance and operating costs attributable to more frequent membrane cleaning and replacement (Lee et al. 2004; Kim et al. 2006; Lee et al. 2009). Moreover, most of the literature in the past two decades focused on fouling rather than cleaning, although a fouling problem may actually be a cleaning problem. Considerable progress has been executed in understanding the interactions between foulants, membrane and operating conditions (Li et al. 2002).

Pretreatments such as coagulation, adsorption, and ozonation are usually utilized before membrane filtration to minimize fouling problems (Chen et al. 2007). Among these, chemical coagulation is the most common one because of its relatively low cost and ease of application (Pikkarainen et al. 2004). Factors that affect coagulation performance and characteristics of membrane fouling include coagulant types, coagulation mechanisms, mixing conditions, adding dosages, and pH (Choi and Dempsey 2004; Muthulumaran et al. 2004).

Although pretreatments might have been employed to minimize fouling, most membrane cleaning techniques are still practically inadequate for membrane filtration systems. Typical methods of membrane cleaning that have been used in industrial applications are forward flushing (spiral wound and tubular) and backwashing (hollow fiber), which are useful with colloidal suspensions (Li et al. 2002). In the mean time, other techniques, such as hydraulic, chemical, mechanical, and electrical cleaning processes, were also utilized to mitigate fouling problems (Lammien et al. 2004; Chen et al. 2007). However, disadvantages of these techniques including

[1]Assistant Professor, Dept. of Environmental Engineering and Science, Chia Nan Univ. of Pharmacy and Science, 60, Erh-Jen Rd., Sec.1, Jen-Te, Tainan, 71710, Taiwan.

[2]Researcher, Disaster Prevention and Water Environment Research Center, National Chiao Tung Univ., 1001 Univ. Road, Hsinchu, 300, Taiwan.

[3]M.S. Student, Dept. of Environmental Engineering and Science, Chia Nan Univ. of Pharmacy and Science, 60, Erh-Jen Rd., Sec.1, Jen-Te, Tainan, 71710, Taiwan.

[4]M.S. Student, Dept. of Chemical Engineering, Univ. of Philippines-Diliman, Quezon City, 1101, Philippines.

[5]Assistant Professor, Dept. of Environmental Engineering and Science, Chia Nan Univ. of Pharmacy and Science, 60, Erh-Jen Rd., Sec.1, Jen-Te, Tainan, 71710, Taiwan (corresponding author). E-mail: cckanev@mail.chna.edu.tw

Note. This manuscript was submitted on November 10, 2010; approved on April 11, 2011; published online on April 13, 2011. Discussion period open until August 1, 2012; separate discussions must be submitted for individual papers. This paper is part of the ***Journal of Environmental Engineering***, Vol. 138, No. 3, March 1, 2012. ©ASCE, ISSN 0733-9372/2012/3-337–343/$25.00.

noncontinuous operation, high chemical costs, waste disposal problems, potential danger of electrolysis, and high capital cost, have limited their field applications.

Ultrasound, a sound wave traveling through a medium at a frequency above 18 kHz, has been considered as an effective technique for membrane cleaning in the past decade. Cavitation phenomenon from ultrasonication can be defined as the formation, growth, and implosion of bubbles, and it can be utilized as an effective energy in fouling elimination. It is widely believed that ultrasonic cavitation, acoustic streaming, ultrasonic-induced vibration of membrane, and ultrasonic heating are the main causes for the enhancement (Zhu and Liu 2000; Lamminen et al. 2004; Muthulumaran et al. 2004). Recently, a number of researchers have demonstrated the effective use of ultrasound for cleaning fouled membranes or for increasing permeate flux of membranes. Lamminen et al. (2004) have illustrated that ceramic membranes were effectively cleaned using ultrasound at frequencies from 70 kHz up to 620 kHz without damaging the membranes. Increases in power intensity of the ultrasonic system increased the cleaned flux ratio. This increase was attributed to an increase in the number of cavitation bubbles and an increase in acoustic energy in the system. However, few mechanistic models have been proposed to explain the ultrasonic enhancement on the membrane separation processes. Lim and Bai (2003) indicated that the particles that blocked the membrane pores were not effectively removed by ultrasound assisted cleaning methods. Therefore, a better understanding on the floc characteristics from various coagulation mechanisms in connections with permeate flux, membrane fouling, and ultrasonic cleaning efficiency is warranted.

This study investigated the extent of membrane fouling from different precoagulation processes and their removals by ultrasound energy. Specifically, it was aimed (1) to determine the optimal alum doses in producing different coagulation mechanisms, named electrostatic patch effect (EPE), charge neutralization (CN), and sweep flocculation (SW); (2) to characterize the flocs from EPE, CN, and SW mechanisms based on their particle diameter, floc strength, and fractal dimension; (3) to develop the plausible mechanisms of precoagulation processes with regards to intrinsic membrane, irreversible fouling and cake resistances; and (4) to determine the cleaning efficiency of fouled PTFE membranes by ultrasound energy.

Materials and Methods

Preparation of Synthetic Raw Water

The synthetic raw water (SRW) was prepared by mixing 1 g of bentonite (Sigma-Aldrich) in 1 L of tap water at 200 rpm for 1 h. The turbidity of the SRW was measured by using a Hach 2100P turbidimeter to be 200 ± 10 NTU.

Preliminary Study for Different Coagulation Mechanisms

Jar-tests were carried out to produce feed waters of different characteristics for membrane filtration. Doses of aluminum sulfate (0.5, 1, 3, 5, 7, 10, and 15 mg/L as Al) were varied to determine the most suitable coagulant concentration for each coagulation mechanism.

Two liters of prepared SRW was used for coagulation and flocculation. The pH was controlled at 7 0.3 using 0.1 N HCl and 0.1 N NaOH. Subsequent to the addition of aluminum sulfate, the mixture was agitated at 200 rpm for 1 min ($G = 350\ s^{-1}$) followed by flocculation at 30 rpm for 20 min ($G = 25\ s^{-1}$). Flocs were allowed to settle for 30 min and were then collected.

In the precoagulation, different coagulation mechanisms, including EPE, CN, and SW, were observed. It was concluded that the EPE mechanism occurred at 1 mg/L of Al wherein the turbidity of the SRW was significantly reduced from 200 to 1.04 NTU. The CN and SW mechanisms took place at 5 and 10 mg/L of Al with zeta potential and residual turbidity of almost 0 mV and 0.49 NTU and +1.66 mV and 0.98 NTU, respectively. The tests of EPE, CN, and SW coagulation mechanisms were called as the EPE, CN, and SW tests in this study.

Floc Characteristics

Characteristics of the flocs collected from the EPE, CN, and SW tests were evaluated. The flocs were characterized on the basis of their particle size, fractal dimension, and floc strength. The particle size (d_{50}) was determined using a particle size analyzer (Mastersizer 2000, Malvern, UK). The fractal dimension (D_f) was calculated by adding unity to the slope of the log-log plot of the particle size and settling velocity. The floc strength (γ) was the regression slope of floc size (d_{50}) and mixing intensity (G).

Membranes

Previous physical analysis showed that polytetrafluoroethylene (PTFE) membrane could withstand the ultrasound irradiation. The PTFE membrane with a nominal pore size of 0.5 μm and an effective area of $1.96 \times 10^{-3}\ m^2$ was used as the microfilter (MF) membrane in this study based on the particle size distribution of the prepared SRW. Prior to use, the PTFE membrane was soaked in citric acid for 30 min and was then washed with deionized water.

Experimental SetUp

The schematic diagram of the dead-end microfiltration set-up is shown in Fig. 1. The set-up was composed of a feed reservoir, the membrane, a pump, a permeate tank, an electronic scale, and an ultrasonic probe. The feed reservoir with a volume of 20 L was used to contain the feed water. The feed water was pumped to the permeate tank by passing through the PTFE membrane. The microfiltration was operated at a transmembrane pressure of 85 kPa. The permeate tank was placed on the electronic scale (XB 4200C, Precisa, Switzerland) that was connected to a computer that recorded the mass of cumulative permeate.

The ultrasonic probe (Sonicator 3000, Misonix) provided physical vibration to clean the cake formed on the surface of the membrane. It was operated at a constant frequency of 20 kHz and 50 W power.

Dead-End Microfiltration

Fifteen liters of precoagulated SRW were fed to the dead-end membrane filtration set-up. A series of five MF tests were conducted. For each test, the feed water was subjected to the MF process for 15 min followed by 1.5 min ultrasonic cleaning.

Analysis of Membrane Fouling Resistances

Membrane fouling resistances were evaluated using the resistance-in-series model (Bae and Tak 2005; Chang and Lee 1998)

$$J = \frac{\Delta P}{\eta R_t} \tag{1}$$

in which J = permeate flux (m^3/m^2-s); ΔP = transmembrane pressure (Pa); η = viscosity of the permeate (Pa-s); and R_t = total resistance (m^{-1}), which can be calculated using Eq. (2):

J. Environ. Eng. 2012.138:337-343.

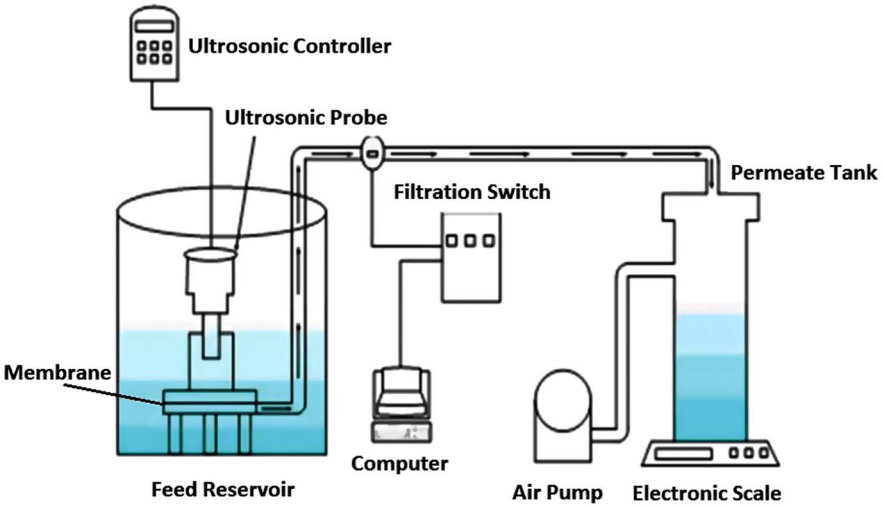

Fig. 1. Schematic diagram of cut-off MF device

$$R_t = R_m + R_f + R_c \quad (2)$$

in which R_m = intrinsic membrane resistance (m^{-1}); R_f = irreversible fouling resistance caused by pore blocking in the membrane pores and on the membrane surface (m^{-1}); and R_c = resistance of the cake formed on the surface of the membrane (m^{-1}).

The R_m, R_f and R_c can be computed using Eqs. (3)–(5):

$$J_{iw} = \frac{\Delta P}{\eta R_{iw}} \quad (3)$$

$$J_{fw} = \frac{\Delta P}{\eta R_{fw}} - R_m \quad (4)$$

$$J_{ss} = \frac{\Delta P}{\eta R_{ss}} - R_m - R_f \quad (5)$$

in which J_{iw} = initial water flux (m^3/m^2-s), which was determined by filtering deionized water until constant flux was achieved; J_{fw} = final water flux (m^3/m^2-s), which was evaluated by passing deionized water through the fouled membrane after removing the cake formed on the membrane surface; and J_{ss} = steady state flux (m^3/m^2-s), which was determined when the flux of the membrane was almost constant or not changing.

Fouled Membranes Examination

The membranes after cleaning at the end of each test were subjected to surface observation using a scanning electron microscope (SEM S-4800, Hitachi, Japan).

Results and Discussion

Precoagulation with Aluminum Sulfate

Characteristics of Flocs from Different Coagulation Mechanisms

The flocs collected from different coagulation mechanisms were characterized on the basis of their particle sizes, fractal dimensions, and floc strengths. These parameters are summarized in Table 1. The EPE test produced the smallest particle size followed by the CN and SW tests. As mentioned earlier, EPE, CN, and SW occurred at 1, 5, of Al, respectively. The increasing size of the flocs from the EPE to CN to SW is associated with the increasing alum dose. According to Wu et al. (2009), floc size increases as the alum dose increases because precipitates form on the surface of the particle and in the solution. A particle collides with other particles to form precipitation. More and more precipitations result in the formation of larger flocs.

Table 1. Floc Characteristics under Different Coagulation Mechanisms using Aluminum Sulfate as Coagulant

Coagulation mechanism	d_{50} (μm)	γ	D_f
EPE	39.54	0.262	2.285
CN	56.57	0.298	2.109
SW	58.90	0.310	1.973

As shown in Table 1, the EPE test also produced the most compact and strongest flocs based on its fractal dimension (D_f) and floc strength (γ). Fractal dimension indicates the structure of the floc or the packing of the aggregates. Flocs with high fractal dimension generate denser flocs that are harder to break compared with the flocs with low fractal dimension. Moreover, stronger flocs have lower floc strength values. Floc size and floc strength have an inverse relationship with fractal dimension. Thus, the SW test produced the largest particle but the weakest and the loosest flocs.

Preliminary Filtration Test under Different Coagulation Mechanisms

The effects of coagulation mechanisms on the permeate flux were evaluated in this study. Fig. 2 shows the declines of the permeate fluxes under three coagulation mechanisms and the blank test. As expected, the blank test showed the most rapid flux decline, and the membrane pores were readily blocked by the particles. The precoagulated SRW under all three coagulation mechanisms reduced the rate of flux decline. The EPE test yielded the slowest flux decline rate. As previously mentioned, the EPE best generated the smallest but the strongest and the most compact flocs. In the EPE mechanism, although the negative charges on some particles are neutralized, repulsion between particles will result in forming filtration cake with larger pore size on membrane surface that cause less flux decline. The SW test produced the largest but the weakest and the most loosely packed flocs in which the particles are surrounded by large amounts of $Al(OH)_3$ coagulants to perform cosedimentation effect, and it will result in forming filtration cake with smaller pore

J. Environ. Eng. 2012.138:337-343.

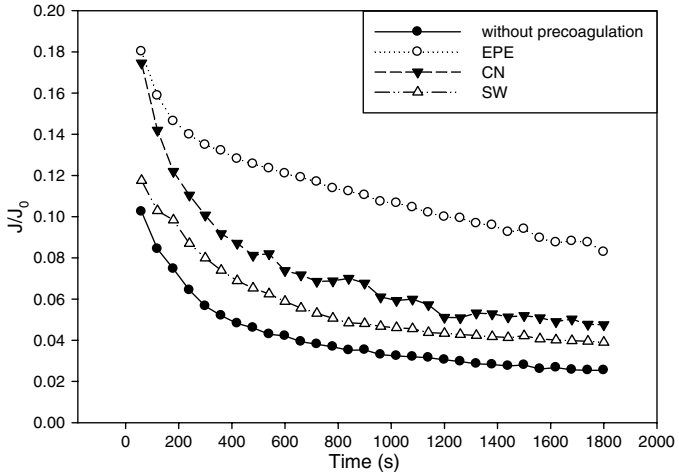

Fig. 2. Membrane flux at different coagulation mechanisms using aluminum sulfate as coagulant

sizes on the membrane surface, causing rapid flux decline. Our results show that coagulation pretreatment improves the permeate flux of the membrane. The permeate flux is enhanced in the order of EPE > CN > SW.

Ultrasonic Cleaning

Five MF and ultrasonic cleaning cycles were performed to determine the effect of ultrasonic cleaning on the initial flux and flux recovery under different coagulation mechanisms. Each cycle was composed of 15 min MF process and 1.5 min ultrasonic cleaning at 20 kHz frequency and 50 W power. Fig. 3 illustrates the declines of the permeate fluxes for the five MF and ultrasonic cleaning cycles, and Table 2 shows the percent flux recoveries after the ultrasonic cleaning.

The percent flux recoveries in all tests, including the blank test, decreased after each cycle. Ultrasonic energy was limited to the removal of the foulants on the membrane surface. As the number of filtration and ultrasonic cleaning cycle increased, the amount of particles blocking the membrane pores also increased, which resulted in decrease in the percent flux recovery. Moreover, among all the tests, the SW test illustrates the highest flux recovery. Because the SW test produced the largest flocs, few membrane pores were blocked by larger particles, where cake was mostly formed on the membrane surface. The cavitation by ultrasound has sufficient energy to generate high velocity fluid movement to remove the cake on the surface of the polymer membrane. Thus, the percent flux recovery increased as the particle size of flocs increased.

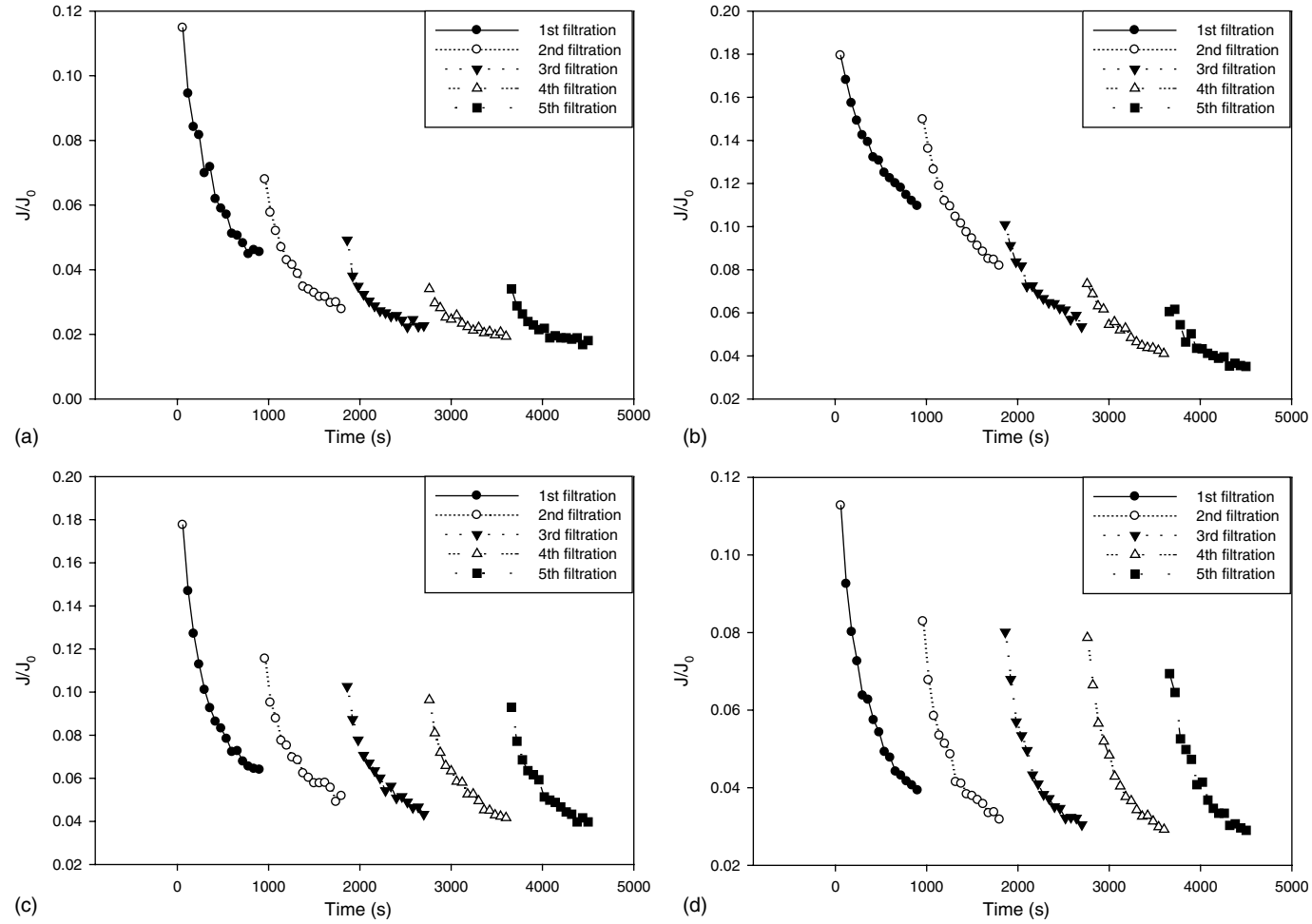

Fig. 3. Flux changes after precoagulation filtration with aluminum sulfate combined with ultrasonic cleaning: (a) without coagulation mechanism; (b) EPE mechanism; (c) CN mechanism; (d) SW mechanism

J. Environ. Eng. 2012.138:337-343.

Table 2. Flux Recovery after MF and Ultrasonic Cleaning Cycle under Different Coagulation Mechanisms

MF cleaning cycle	Flux recovery percent (%)			
	Blank	EPE	CN	SW
1	—	—	—	—
2	59.65	83.24	64.97	73.21
3	42.98	56.42	57.63	71.43
4	29.82	40.78	54.24	69.64
5	29.82	33.52	51.98	61.61

Fouling Mechanism

The fouling resistances and mechanisms of the blank and the different precoagulation tests were evaluated. The total resistance (R_t) for each MF and ultrasonic cleaning cycle was calculated using the resistance-in-series model. The total resistances for the blank, EPE, CN, and SW tests were 2.52–6.32 × 107, 1.04–3.26 × 107, 1.79–2.88 × 107, and 2.19–3.94 × 107 m^{-1}, respectively. Blank test showed the highest total resistance, and coagulation pretreatment decreased the total resistance in the MF process.

Fig. 4 shows the distribution ratios of intrinsic membrane (R_m), irreversible fouling (R_f), and cake (R_c) resistances during the tests. In almost all the tests, the R_f decreased whereas the R_c increased as the number of filtration cycle increased. The results imply that the membrane fouling mechanism was predominantly pore blocking, but gradually switched to cake formation. Comparing the results of different tests, the EPE test illustrates the largest R_f ratios (65% ~ 73%), which indicates that pore blocking was the major fouling mechanism in the EPE test. In CN test, the ratio of R_f varied between 44% to 55% and R_c between 38% to 52%. The R_f and R_c ratios showing small differences indicates the combined effects of pore blocking and cake formation. On the contrary, the R_c in the SW test ranged from 50% to 58%, which is larger than 39% to 47% of R_f, which indicates that cake formation was the predominant fouling mechanism. Thus, the smaller but more compact and stronger flocs results in pore blocking, whereas larger, but looser and weaker flocs results in cake formation.

Membrane Surface

The SEM photographs of the fouled and ultrasonic cleaned membranes are shown in Fig. 5. Fig. 5(a) shows the surface morphology of the membrane fouled by the SRW without precoagulation. The membrane was covered by dense foulants. Fig. 5(b) is the surface image of the fouled membrane under the EPE test, which is very different from the blank test (i.e., the interlaced membrane fibers could be seen clearly and several colloids was between the fibers). Figs. 5(c) and 5(d) are the surface images of ultrasonic cleaned membrane surface from the CN and SW tests, respectively. Both show large colloids and a layer of cake on the membrane.

The SEM photographs of the ultrasonic cleaned membranes show the phenomenon of floc blocking between the membrane fibers. Although the smaller and compact flocs may have a larger membrane flux in the early part of filtration, these flocs would block the pores and cause inefficient cleaning, because they were

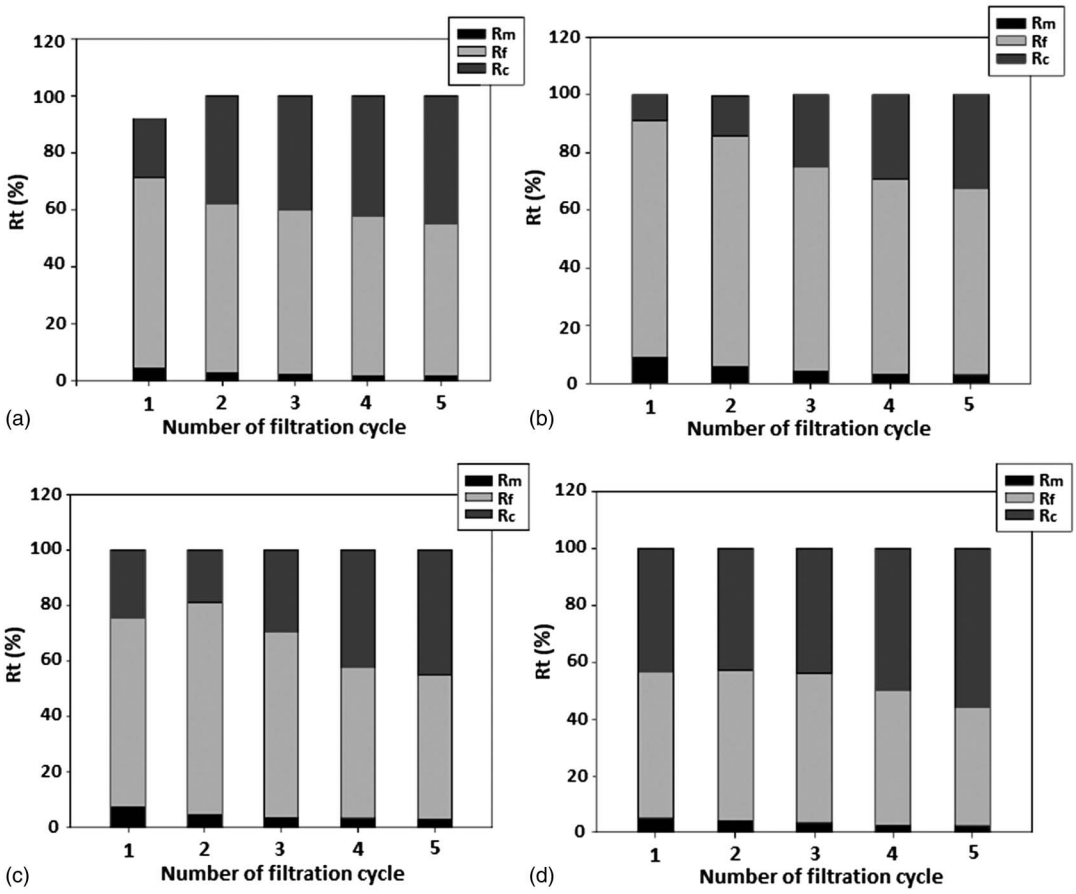

Fig. 4. Resistance ratio variation with filtration-clean loops in different coagulation mechanism tests: (a) blank test without precoagulation; (b) EPE mechanism; (c) CN mechanism; (d) SW mechanism

J. Environ. Eng. 2012.138:337-343.

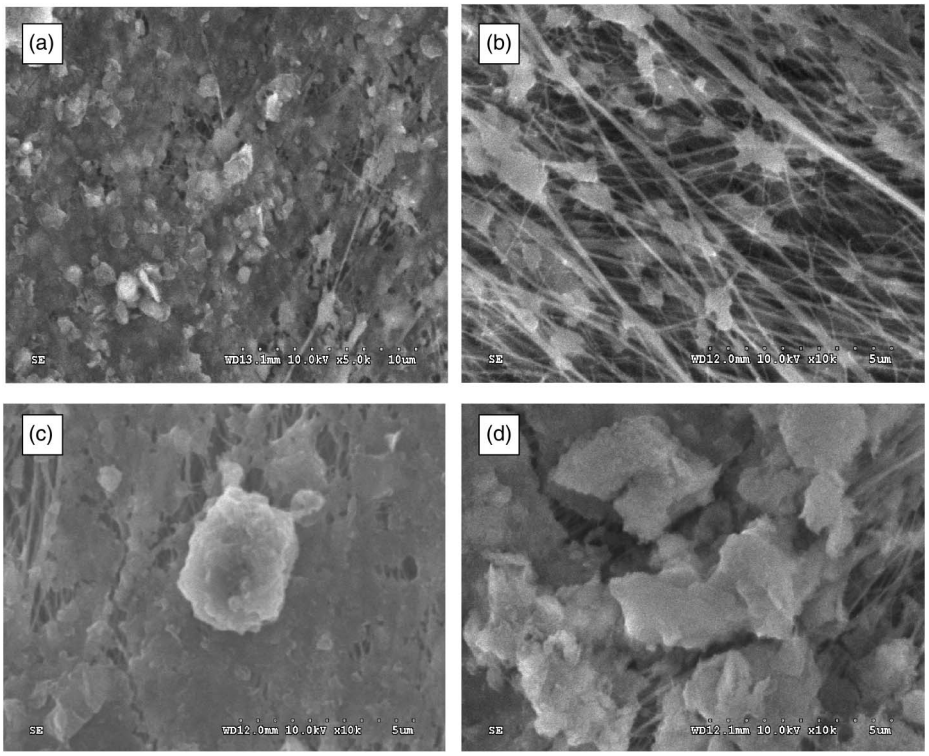

Fig. 5. SEM observation of membrane surface after precoagulation filtration with aluminum sulfate combined with ultrasonic cleaning: (a) no precoagulation; (b) EPE mechanism; (c) CN mechanism; (d) SW mechanism

more difficult to be washed out. Hence, precoagulation with the EPE mechanism would generate more irreversible fouling. The CN mechanism produced flocs with a strength and shape similar to the SW mechanism but larger than that from the EPE mechanism. The larger colloids resulted in larger permeate flux and a better restoration ratio of flux after membrane cleaning. Moreover, the SW mechanism that produced the largest but the looser and weaker flocs had a higher potential in cake formation, where the quick formation of cake resulted in higher R_t and lower permeate flux. However, the formed foulant layer on the membrane surface could really be removed by ultrasonic cleaning as evidenced from good restoration ratios of permeate flux.

Conclusions

Flocs generated from three different coagulation mechanisms differed in size, structure, and strength. EPE mechanism produced the smallest but the densest and the strongest flocs, whereas the SW mechanism generated the largest, but the loosest and the weakest flocs. Differences in floc characteristics resulted in different types of fouling types. The predominant mechanisms of the EPE and SW tests are pore blocking and cake formation, respectively. The CN test is in between pore blocking and cake formation. Precoagulation improved the permeate flux. The permeate flux was enhanced in the sequence of EPE > CN > SW, in which floc fractal dimension increased as the floc strength and particle size decreased. The flux recovery after ultrasonic cleaning decreased in the sequence of SW > CN > EPE. This study evidenced that the different coagulation mechanisms affect the types of fouling of membrane and extent of flux recovery by ultrasonic cleaning.

References

Bae, T. H., and Tak, T. M. (2005). "Interpretation of fouling characteristics of ultrafiltration membranes during the filtration of membrane bioreactor mixed liquor." *J. Membr. Sci.*, 264(1–2), 151–160.

Bergamasco, R., Bouchard, C., Silva, F. V., Reis, M. H. M., and Fagundes-Klen, M. R. (2009). "An application of chitosan as a coagulant/flocculant in a microfiltration process of natural water." *Desalination*, 245(1–3), 205–213.

Chang, I. S., and Lee, C. H. (1998). "Membrane filtration characteristics in membrane-coupled activated sludge system—the effect of physiological states of activated sludge on membrane fouling." *Desalination*, 120(3), 221–233.

Chen, Y., Dong, B. Z., Gao, N. Y., and Fan, J. C. (2007). "Effect of coagulation pretreatment on fouling of an ultrafiltration membrane." *Desalination*, 204(1–3), 181–188.

Choi, K. Y., and Dempsey, B. A. (2004). "In-line coagulation with low-pressure membrane filtration." *Water Res.*, 38(19), 4271–4281.

Kim, H. C., Hong, J. H., and Lee, S. (2006). "Fouling of microfiltration membranes by natural organic matter after coagulation treatment: A comparison of different initial mixing conditions." *J. Membr. Sci.*, 283(1–2), 266–272.

Kweon, J. H., et al. (2009). "Evaluation of coagulation and PAC adsorption pretreatments on membrane filtration for a surface water in Korea: A pilot study." *Desalination*, 249(1), 212–216.

Lamminen, M. O., Walker, H. W., and Weavers, L. K. (2004). "Mechanisms and factors influencing the ultrasonic cleaning of particle-fouled ceramic membranes." *J. Membr. Sci.*, 237(1–2), 213–223.

Lee, B., Choo, K., Chang, D., and Choi, S. (2009). "Optimizing the coagulant dose to control membrane fouling in combined coagulation/ultrafiltration systems for textile wastewater reclamation." *Chem. Eng. J.*, 155(1–2), 101–107.

Lee, N., Amy, G., Crouc, J. P., and Buisson, H. (2004). "Identification and understanding of fouling in low-pressure membrane (MF/UF) filtration by natural organic matter (NOM)." *Water Res.*, 38(20), 4511–4523.

J. Environ. Eng. 2012.138:337-343.

Li, J., Sanderson, R. D., and Jacobs, E. P. (2002). "Ultrasonic cleaning of nylon microfiltration membranes fouled by Kraft paper mill effluent." *J. Membr. Sci.*, 205(1–2), 247–257.

Lim, A. L., and Bai, R. (2003). "Membrane fouling and cleaning in microfiltration of activated sludge wastewater." *J. Membr. Sci.*, 216(1–2), 279–290.

Muthulumaran, S., Yang, K., Sueren, A., Kentish, S., Ashokkumar, M. G. W., and Grieser, F. (2004). "The use of ultrasonic cleaning for ultrafiltration membranes in the dairy industry." *Sep. Purif. Technol.*, 39(1–2), 99–107.

Pikkarainen, A. T., Judd, S. J., Jokela, J., and Gillberg, L. (2004). "Pre-coagulation for microfiltration of an uplandsurface water." *Water Res.*, 38(2), 455–465.

Strathmann, H. (1976). "Membrane separation processes in advanced waste water treatment." *Pure Appl. Chem.*, 46(2–4), 213–220.

Wu, X., Ge, X., Wang, D., and Tang, H. (2009). "Distinct mechanisms of particle aggregation induced by alum and PACl: Floc structure and DLVO evaluation." *Colloids Surf.*, 347(1–3), 56–63.

Zhu, C., and Liu, G. L. (2000). "Modeling of ultrasonic enhancement on membrane distillation." *J. Membr. Sci.*, 176(1), 31–41.

J. Environ. Eng. 2012.138:337-343.